Seismic characteristics of gas hydrate system at the Hydrate Ridge, offshore Oregon

Dhananjay Kumar[#], Mrinal K. Sen*, and Nathan L. Bangs, The University of Texas at Austin
[#] Presently at ChevronTexaco Energy Technology Company, San Ramon, California

This paper was prepared for presentation at the 9th International Congress of The Brazilian Geophysical Society held in Salvador, Brazil, 11-14 September 2005.

Abstract

Seismic wave velocities vary in the presence of gas hydrate and free gas in the sediments. Seismic properties (velocities) of the gas-hydrate bearing sediments allow us to identify the presence of gas hydrates, to study their character, formation and distribution, and to estimate the amount of gas hydrate and/or free gas that may be present in the sediments. Accuracy in the estimation of distribution and saturation of gas hydrates and free gas depends on the interval velocities of P- and S-waves. We have carried out an interactive velocity analysis of P- and converted S-waves in the tau-p (intercept time – ray parameters) domain, which directly gives the interval velocities. This requires multicomponent seismic data. A two-ship seismic experiment was carried out (to record multicomponent seismic data) in summer 2002 at the Hydrate Ridge to map the gas hydrate. Our approach to multicomponent velocity analysis comprises three steps: 1) P-wave velocity analysis, 2) PP to PS event correlation, and 3) S-wave velocity analysis. PP to PS correlation is performed using synthetic seismograms. Observed velocities are matched with modeled velocities to estimate gas hydrate saturation. P- and S-wave velocities are modeled with a "Modified Wood equation" which is a modification of Wood equation with a rock physics model and an empirical relation, respectively. We present results from the multicomponent ocean bottom seismometer data recorded at the Hydrate Ridge, offshore Oregon. The P-wave velocity is found to be more sensitive to the saturation of gas hydrates and free gas than S-wave velocity. Gas hydrate is estimated to be upto 7% of rock volume (12% of pore space). The S-wave velocity does not show an anomalous increase in the hydrate-bearing sediments. Thus we conclude that hydrate does not cement sediment grains enough to affect shear properties. It is more likely that the hydrates are formed within the pore space in this region.

Introduction

Gas hydrate is an ice-like substance that contains low molecular weight gases (mostly methane) in a lattice of water molecules (Sloan, 1998). In marine environments, methane hydrates are usually stable at temperatures in the range of 0^0C to 150^0C, water depth greater than 500 m, and sediment depths up to 300 meters below sea floor. Formation of gas hydrate is favorable in the deeper ocean (methane gas, water and thermodynamic conditions are available), which means huge amount of gas (about 15000 giga tones) may be present in the offshore gas hydrates (Kvenvolden, 1999). Free gas is usually present below the gas hydrates. Hydrates and free-gas make a strong acoustic interface, which is evident in seismic section as a Bottom Simulating Reflector (BSR). Offshore gas hydrates system has got attention from the geoscientist because of its potential to be 1) a drilling hazard, 2) a future energy source, 3) continental slope stability, and 4) a factor affecting global carbon cycle. Many of these relations are not well established, which can be better constrained if distribution and saturation of gas hydrates and free gas are known. Gas hydrates and free-gas are generally detectable with seismic methods (Yuan et al., 1996) since the seismic velocity, in general, increases in the presence of gas hydrates and decreases in the presence of free gas. The velocity also increases if the hydrate content in the pore spaces increases (Hyndman and Spence, 1992). Therefore, seismic velocity has been widely used to estimate the saturation of gas hydrates and free gas (e.g., Lee et al., 1996; Helgerud et al., 1999; Lu and McMechan, 2002). Other methods gives local estimation of gas hydrates using resistivity data from well logs, chloride measurement from core data, infra-red image of cores, and pressure core sampler (Dickens et al., 1997; Trehu et al., 2004).

Hydrate Ridge (HR) is a 25-km long and 15-km wide accretionary ridge in the Cascadia convergent margin (MacKay, 1995) formed as the Juan de Fuca plate subducts obliquely beneath the North American plate (Figure 1). Hydrates and its seismic proxies (BSR, and amplitude blanking) appear to be well developed beneath HR (Trehu et al., 1999). A two-ship seismic experiment was conducted at the HR during summer 2002 with the seismic ship *Maurice Ewing* and the drilling ship *JOIDES Resolution*. The cruise was designed to acquire surface seismic (streamer recording, MCS) and subsurface seismic [Vertical seismic profiles (VSP) and Ocean bottom seismometer (OBS)] data to map the distribution and saturation of gas hydrates which is possible with accurate estimation of elastic properties (P- and S-waves velocities) of gas hydrate- and free gas- bearing sediments.

Seismic velocity analysis is normally performed in the offset-time ($x-t$) domain, which gives root mean square (RMS) velocity. The resultant RMS velocity is converted to interval velocity using the Dix equation (Dix, 1955). Interval velocity can be directly estimated with data analysis in the tau-p (intercept time – ray parameters) domain (Stoffa et al., 1981). We have carried out an interactive velocity analysis for P- and S-waves in the tau-p domain. S-wave in marine setting is a converted shear wave, and can be recorded with multicomponent receivers as OBS, and VSP geometry. We use the OBS data recorded on the HR. Presence of weak anisotropy due to the hydrate veins has been reported by Kumar et al. (2004), however we will consider isotropy model in this study. Once interval velocities are estimated, they are

used to estimate the volumetric saturation of gas hydrates in the rock.

Interval multicomponent velocity analysis

For a layered medium, with source and receiver at the same level and reflector at a depth of Δz, the reflection traveltime t, from source to receiver at a distance of x is given as,

$$t = \tau + px \tag{1}$$

which describes a straight line tangent to the traveltime curves at (t, x), with intercept time τ and slope p (ray parameter). Intercept time is a two-way vertical traveltime ($\tau = 2q\Delta z$), where q is the vertical slowness (inverse of velocity). Seismic data recorded as a function of offset (x) and traveltime (t) can be mapped to the domain of intercept time (τ) and ray parameter (p) (e.g., Stoffa et al., 1981). Each trace in the $\tau - p$ plane corresponds to a ray-parameter. The hyperbolic reflection trajectories in the (x,t) domain map to ellipse in the (τ, p) domain. The $\tau - p$ trajectories of the reflected P- and converted S-waves are given (Bessonova et al., 1974), respectively as,

$$\tau_P(p) = 2\tau_P^0\sqrt{1 - p^2V_P^2} \tag{2}$$

and

$$\tau_S(p) = \tau_P^0\sqrt{1 - p^2V_P^2} + \tau_S^0\sqrt{1 - p^2V_S^2}\,, \tag{3}$$

where τ_P^0 and τ_S^0 are one-way vertical traveltimes, and V_P and V_S are velocity of P- and S-waves, respectively. It is evident from equation (3) that for S-wave (PS-wave), incident and reflected time correspond to P- and S-wave traveltime, respectively. In ocean-bottom recording, first arrivals are direct P-wave (one-way P-wave traveltime) and it must be taken are of when using the above equations for the data analysis. Velocity analysis steps are discussed in next section assuming 1D isotropic model.

Interval velocity analysis steps

Velocity analysis for V_P and V_S requires multicomponent recording, where hydrophone (or vertical) and radial geophone are designed to record the P- and S-waves, respectively. Steps for interval velocity analysis are: 1) P-wave velocity estimation using equation (2), 2) mapping of P- (PP) and S-wave (PS) reflection event, and 3) S-wave velocity estimation using equation (3). Step 1 is trivial. After P-wave analysis, S-wave reflections are identified in the radial geophone data corresponding to the P-wave reflections in the hydrophone data. Matching of P- and S-wave reflection for a reflector is performed with the help of traveltime table and synthetic seismogram. Traveltime for S-wave (PS-wave) is estimated for a reflector using V_P from previous step and V_S from sonic log (or model value). The traveltime table helps identify various wave types in a seismogram. Synthetic seismogram is created to match the S-wave arrival at the estimated time; this way S-wave reflection arrival is identified for each reflector. Matching of reflectors can be performed in $x - t$ and/or $\tau - p$ domain. Figure 2a shows the identification and matching of S-wave event for a corresponding P-wave event between real and synthetic radial geophone data for an OBS (#19) (receiver gather). At the same OBS location, Figure 2b shows the mapping of P- and S-waves reflections on hydrophone and radial component data, respectively. It is possible that S-wave response is weak for some reflectors; if P- to S-wave conversion is weak and then it require geological interpretation to map PP to PS data. Once PS reflections are identified on the radial geophone data, interactive interval velocity analysis is performed in the tau-p domain (using equation 3) for S-wave velocity (Kumar, 2005). Figure 3 shows the P- and S-wave velocities estimated from multicomponent OBS data. Once seismic velocities are available we are ready for estimation of gas hydrate saturation.

Gas hydrate saturation estimation

Seismic wave velocities are greatly influenced by the presence of gas hydrate and free gas in the sediments (e.g., Yuan et al., 199). P- and S-wave velocity information (anomalous with respect to a background velocity) can be used to estimate the gas hydrate and free gas distribution and saturation. This requires a relation between hydrate (and/or free gas) fraction in the sediments and the elastic properties (Vp and Vs). Several authors have presented relationships between velocity and gas hydrate concentration, which can be broadly categorized in two forms: 1) Wyllie's (1958) time average or Wood's (1941) relation (e.g., Lee et al., 1996), and 2) rock physics based effective medium modeling (e.g., Helgerud, et al., 1999). The first relation is empirical and simple, and the second method is more physical but difficult to implement. Rock physics based method requires information about the type of hydrate model (cement, part of matrix frame, or floating in the pore spaces), critical porosity of the matrix, effective pressure, and coordination number (of hydrate crystal) which are again not trivial. Here we used a simple and meaningful formulation developed by Kumar (2005). This formulation modify the Wood equation with a rock physics model for calculation of P-wave velocity in hydrate-bearing sediments, and call it a "Modified Wood equation". This method uses volumetric averaging of compliances.

Table 1 lists all the parameters and its values used in the seismic velocity estimation. Clay (80%) and Quartz (20%) constitute the mineral grains. For the estimation of gas hydrates and free gas saturation in a layer, we match theoretical and observed velocities. Theoretical velocities are calculated with modified Wood equation for P-wave and an empirical relation for S-wave (Kumar, 2005), and observed velocities (Figure 3) are found from multicomponent velocity analysis as discussed above. Matching observed and calculated velocities at the OBS stations produce 1D saturation values. We interpolated and smoothed the 1D saturation values at OBS sites to produce a 2D profile of hydrate saturation, where maximum hydrate saturation is about 7% of the rocks volume (which is 12% of the pore space and 15% of solid phase). This hydrate saturation estimation agrees with the saturation derived from cores and log data (Trehu et al., 2004). Our saturation estimation deviates from the

saturation derived from core and log data at the south summit in the first 10m below seafloor (Trehu et al., 2004), as our estimation is comparatively lower. This discrepancy is possibly due to the presence of free gas at that position (10m below seafloor) which affects the P-wave velocity significantly and therefore reduces hydrate saturation estimation; also from velocity analysis such a fine resolution is not available.

Interpretation of the results

Analysis of converted S-waves on multicomponent seismic data is not a trivial task; it depends on the quality of the data, accuracy of the P-wave velocity and correlation of P- to S-wave reflection events. These require knowledge of geological settings of area and constraints from other independent sources. The S-wave velocity is estimated for a reflection event for which the P-wave reflection event is known. Since P- and S-wave reflectivity for a layer-interface are not the same, for some reflectors, correlation of events on P- and S-wave data are not trivial. Synthetic seismograms and traveltime tables helped in event correlation. Finally we match the reflectors on P- and S-wave data in depth. The S-wave velocity analysis at the south summit and the slope basin site are well constrained by the sonic logs and geological information. However, since S-waves propagate nearly vertically to the receivers, there is not much angle coverage by the reflected S-wave (incident wave is P-wave) and therefore the NMO (normal moveout) application (curve fitting) is not very sensitive to velocity variations. Fortunately, sonic logs are available at two locations.

The S-wave velocity in the hydrate-bearing sediments (from the seafloor to the BSR) does not show anomalous increase like the P-wave velocity (Figure 3). We interpret that the hydrate does not cement sediment grains enough to affect shear properties significantly. It is more likely that hydrates form within the pore space as part of the sediments. This is also observed in the drilling data (Trehu et al., 2003). This interpretation reduces the effect of gas hydrate as a possible cause of slope stability and slope failure, since even if hydrate dissociates (resulting into free gas and water), the shear strength of accompanying sediments will not decrease significantly which will prevent the sediments flow.

The P- and S-wave velocities are effective in identification of hydrate-bearing zones and quantification of the hydrate saturation. The lower P-wave velocity and unchanged S-wave velocity below the BSR (and close to the seafloor at the south summit) (Figure 3) indicate the presence of free gas, which supports the fluid migration mechanism from below the BSR to the seafloor. Free gas present below the BSR can move up if they are oversaturated (to overcome the capillary forces) and/or in the presence of fluid path. On the Hydrate Ridge, our results indicate that P-wave velocities are more sensitive than the S-wave velocities on the variation of gas-hydrate and free-gas saturation, This new velocity calculation formulation is realistic and simple to implement, and can be used to remotely estimate hydrate saturation. However, in areas where both free-gas and gas-hydrates are present (as in the case of about 10m below the seafloor at the south summit) this formulation is not accurate. Also for better resolution of hydrate saturation higher resolution seismic velocities are required, which is possible with multicomponent data recorded with closely spaced receivers (i.e., Ocean Bottom Cable data).

Hydrate saturation estimated at the Hydrate Ridge is up to 7% of the bulk rock volume (which is 12% of the pore space and 15% of the solid phase). This saturation of hydrates in the sediments are probably not sufficient to seal the free gas below BSR level, however it will restrict the fluid motion upward through hydrate-bearing sediments. Two other reasons for the presence of free gas below BSR are: 1) thermodynamic condition below the BSR (i.e., high temperature) is not favorable for the hydrates and they are in the free gas form, and 2) saturation of free gas below BSR is low (about 2-5%) (known from the drilling result) in that case the capillary forces will not allow the free gas to move (Clennell et al., 1999). From the estimated hydrate saturation and the free gas saturation known from the drilling, it is more likely that presence of hydrate is not the only reason to keep the free gas below BSR level, but it does prohibit the fluid flow through hydrate-bearing sediments.

Discussions and conclusions

The S-wave velocity analysis requires accurate measurement of P-wave velocity and correlation of P- and S-wave reflection events. Event correlation between P- and S-wave data is performed with the help of synthetic seismograms. In many situations, the event correlation is not trivial and it requires constraints from other sources. I used sonic and dipole sonic logs available at the two locations to constrain the event correlation and S-wave velocity estimation. The P- and S-wave velocities together confirm the presence of free-gas below the BSR and in the shallow zones at the south summit. The derived S-wave velocity profiles are monotonically increasing functions of depth within the hydrate-bearing sediment, which suggests that hydrates are not cementing the matrix grains enough to increase the shear properties significantly. It is likely that the hydrates are within the pore space as part of the sediments. we used a modified Wood equation, which includes rock physics based saturation effects of hydrates, for calculation of seismic velocities in gas-hydrate-bearing sediments, and is appropriate for the Hydrate Ridge area. The mapping of the derived seismic velocities to the gas hydrates saturation at the HR results in the maximum hydrate saturation of 7% of the bulk rock volume (12 % of pore space). Because the hydrate occupies just small portion of the pore space, it is not sufficient to seal the free gas below BSR, and free gas is present likely due to the thermodynamic condition and capillary forces. The estimation of hydrate saturation agrees with drilling data, except at the south summit (up to 10m down from the seafloor) where free gas migrates up into the hydrate stability zone

Acknowledgements

We thank Robert H Tatham and Paul L Stoffa at the University of Texas at Austin for discussions on multicomponent velocity analysis and rock physics models. This project is funded by the National Science Foundation.

References

Bessonova, E. N., Fishman, V. M., Ryaboyi, V., Z., and Stinikova, G. A., 1974, The Tau method for inversion of travel times-I. Deep seismic sounding data: Geophys. J. R. astr. Soc., **36**, 377-398.

Clennel, M. B., Hovland, M., Booth, J. S., Henry, P., and Winters, W. J., 1999, Formation of natural gas hydrates in marine sediments 1: Conceptual model of gas hydrate growth conditioned by host sediment properties: J Geophys. Res., **104**, 22985-23003.

Dickens, G. R., Paull, C. K., Wallace, P., and the ODP Leg 164 Scientific party, 1997, Direct measurement of in situ methane quantities in a large gas hydrate reservoir. Nature, **385**, 427-428.

Dix, C. H., 1955, Seismic velocities from surface measurements: Geophysics, **20**, 68-86.

Helgerud, M. B., Dvorkin, J., Nur, A. Sakai, A., and Collett, T., 1999, Effective wave velocity in marine sediments with gas hydrates: Effective medium modeling: Geophys. Res. Lett., 26, 2021-2024.

Hyndman, R. D., and Spence, G. D., 1992, A seismic study of methane hydrate marine bottom simulating reflectors: J. Geophys. Res., 97, B5, 6683-6698.

Kumar, D., 2005, Analysis of multicomponent seismic data from the Hydrate Ridge, offshore Oregon: PhD thesis, The university of Texas at Austin .

Kumar, D., Sen, M. K., and Bangs, N. L., 2004, P-wave seismic anisotropy on Hydrate Ridge: SEG Denver, Expanded Abstract, 159-162.

Kvenvolden, K. A., 1999, Potential effects of gas hydrate on human welfare: Proceedings of the National Academy of Science, USA, **96**, 3420-3426.

Lee, M. W., Hutchinson, D. R., Collett, T. S., and Dillon, W. P., 1996, Seismic velocities for hydrate-bearing sediments using weighted equation: J. Geophys. Res., 101, 20347-20358.

Lu, S., and McMechan, G. A., 2002, Estimation of gas hydrate and free gas saturation, concentration, and distribution from seismic data: Geophysics, 67, 582-593.

MacKay, M. E., 1995, Structural variation and landward vergence at the toe of the Oregon accretionary prism: Tectonics, 14, 1309-1320.

Sloan, E. D. Jr., 1998, Clathrate Hydrates of Natural Gases: Marcel Dekker, New York .

Stoffa, P. L., Buhl, P., Diebold, J. B., Wenzel, F., 1981, Direct mapping of seismic data to the domain of intercept time and ray parameter – A plane-wave decomposition: Geophysics, **46**, 255-267.

Trehu, A. M., Torres, M. E., Moore, G. F., Suess, E., and Bohrmann, G., 1999, Temporal and spatial evolution of a gas-hydrate-bearing accretionary ridge on the Oregon continental margin: Geology, 27, 939-942.

Trehu, A. M., Bohrmann, G., Rack, F. R., Torres, M. E., and Leg 204 Scientific Party, 2003, Proceedings of the Ocean Drilling Program, Initial Reports, 204, online at: http://www-odp.tamu/publications/204_IR/204TOC.HTM.

Trehu, A. M. et al., 2004, Three-dimensional distribution of gas hydrate beneath southern Hydrate Ridge: constraints from ODP Leg 204: Earth Planet. Sci. Let., 222, 845-862.

Yuan, T., Hyndman, R. D., Spence, G.D., and Desmons, B, 1996, Seismic velocity increase and deep-sea gas hydrate concentration above a bottom-simulating reflector on the northern Cascadia continental slope: J. Geophys. Res., 101, 13655-13671.

Wood, A. B., 1941, Text book of sounds, 578 pp., Macmillan, New York .

Wyllie, M. R., Gregory, A. R., and Gardner, G. H. P., 1958, An experimental investigation of factors affecting elastic wave velocities in porous media: Geophysics, 23, 459-493.

Constituents	Volume (%)	K (GPa)	G (GPa)	ρ (g/cm^3)
Clay	80	20.9	6.85	2.58
Quartz	20	36.6	45.0	2.65
Gas hydrate	S_h	7.9	3.3	0.90
Water	S_w	2.25	0	1.0
Methane gas	S_g	0.11	0	0.23

Table 1. Parameters used in the estimation of gas hydrate and free gas saturation: S_h is the volumetric fraction of hydrates in the rock, and water (S_w) and methane gas (S_g) making the fluid (i.e., $S_w + S_g = 1$). Data are from Helgerud et al. (1999) and Lee et al. (1996) (*).

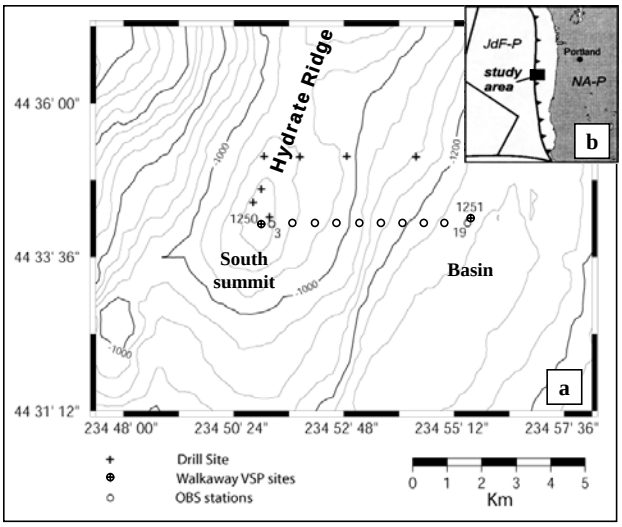

Fig. 1. Bathymetry map (contours in m) on the Hydrate Ridge of the Cascadia convergent margin, offshore Oregon (a). Location of two sites, south summit and basin site are marked. There are seven other OBSs between these two sites, and one OBS is left to OBS 3. Inside map (b) shows subduction of the Juan de Fuca plate (JdF-P) beneath the North American plate (NA-P).

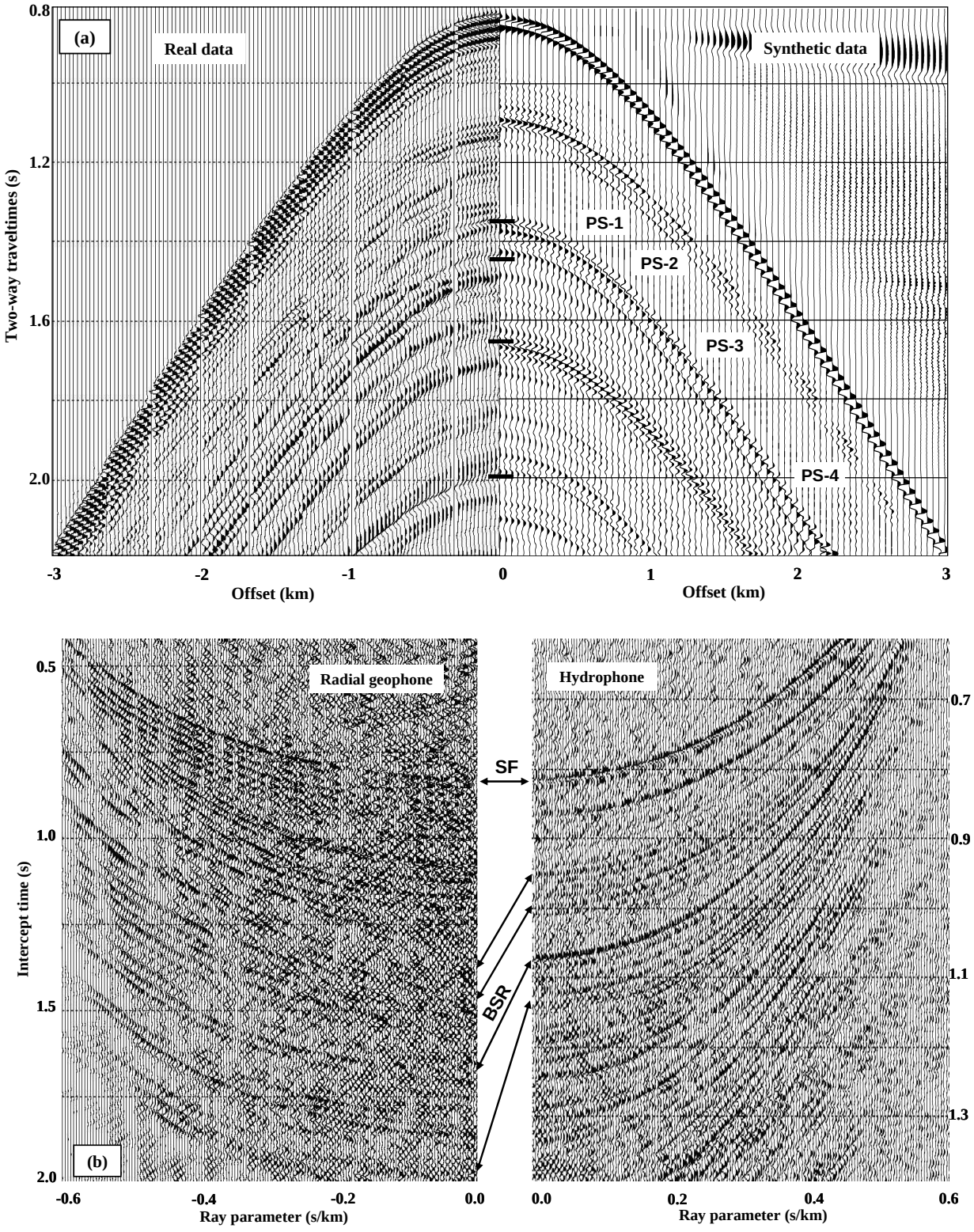

Fig. 2. Matching converted wave (PS) arrivals on the radial geophone data in the $x-t$ domain between real and synthetic data (a) and Mapping of P- and S-wave arrivals in the tau-p domain on the hydrophone and the radial geophone data, respectively (b) for a S-N profile over OBS station 19. Seismic velocities used in the synthetic seismogram (a) are derived from sonic log close to this OBS location (#19), and Reflectivity method is used to generate the seismogram. The ratio of P- and S-wave velocities varies from 6.8 near the SF (seafloor) to 4.8 near the fourth (last) reflector.

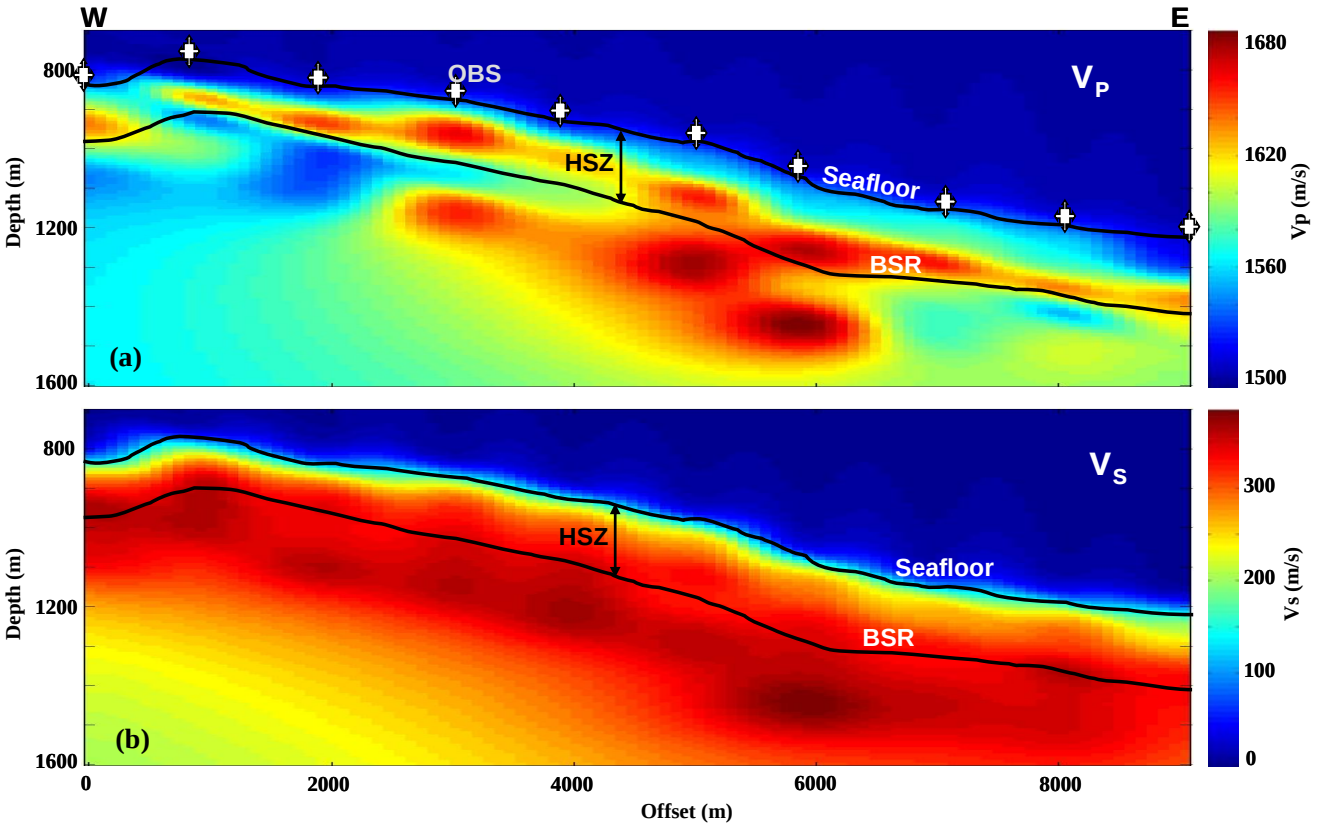

Fig. 3. P- and S-wave interval velocities estimated from the multicomponent OBS data. Estimated 1D velocity profiles are interpolated to derive a smooth 2D profile. P-wave velocity is higher above BSR due to the presence of gas hydrates and is lower below BSR due to the presence of free gas. S-wave velocity is not abnormally high above BSR (like P-wave velocity) which implies that presence of hydrate is not increasing shear strength of the gas-hydrate bearing sediments, and therefore gas hydrates are unlikely to cement the sediment grains.

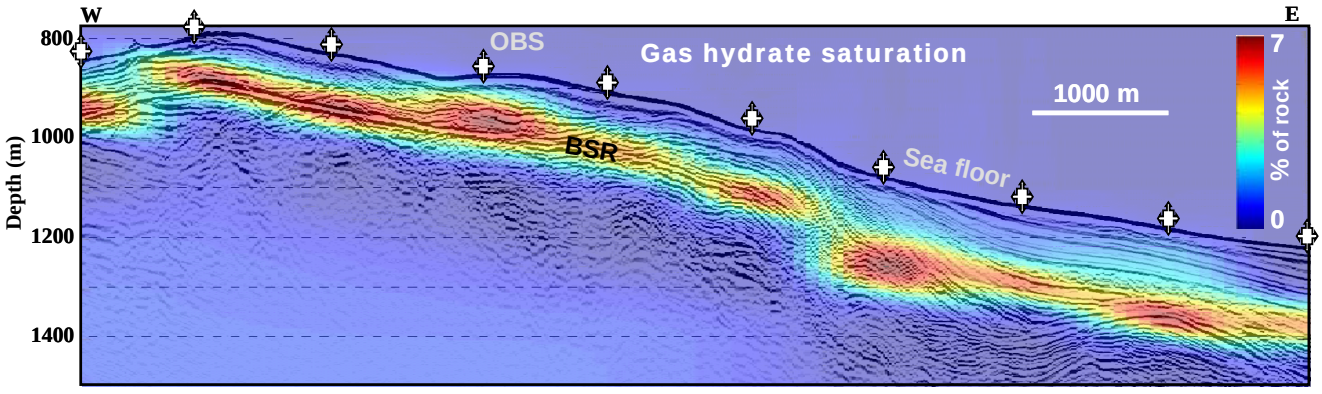

Fig. 4. Gas hydrate saturation (as volumetric saturation of total rock across the south summit (W-E) on the Hydrate Ridge. Saturation estimation is performed by matching the observed velocities with the calculated velocities. Profile of hydrate concentration has been plotted over streamer data (HR #4). BSR marks the base of gas-hydrate stability zone. Hydrate saturation is higher on the south summit (westward) than on the slope basin side.